The chloroplast metalloproteases VAR2 and EGY1 act synergistically to regulate chloroplast development in Arabidopsis

Received for publication, November 11, 2019, and in revised form, December 9, 2019 Published, Papers in Press, December 13, 2019, DOI 10.1074/jbc.RA119.011853

Yafei Qi (齐 亚飞)[1], **Xiaomin Wang** (王 晓敏)[1], **Pei Lei** (雷 霈), **Huimin Li** (李 慧敏), **Liru Yan** (闫 丽如), **Jun Zhao** (赵 军), **Jingjing Meng** (孟 晶晶), **Jingxia Shao** (邵 景侠), **Lijun An** (安 丽君), **Fei Yu** (郁 飞), **and Xiayan Liu** (刘 夏燕)[2]

From the State Key Laboratory of Crop Stress Biology for Arid Areas and College of Life Sciences, Northwest A&F University, Yangling, Shaanxi 712100 China

Edited by Joseph M. Jez

Chloroplast development and photosynthesis require the proper assembly and turnover of photosynthetic protein complexes. Chloroplasts harbor a repertoire of proteases to facilitate proteostasis and development. We have previously used an Arabidopsis leaf variegation mutant, *yellow variegated2* (*var2*), defective in thylakoid FtsH protease complexes, as a tool to dissect the genetic regulation of chloroplast development. Here, we report a new genetic enhancer mutant of *var2*, *enhancer of variegation3–1* (*evr3–1*). We confirm that *EVR3* encodes a chloroplast metalloprotease, reported previously as ethylene-dependent gravitropism-deficient and yellow-green1 (EGY1)/ammonium overly sensitive1 (AMOS1). We observed that mutations in *EVR3*/*EGY1*/*AMOS1* cause more severe leaf variegation in *var2–5* and synthetic lethality in *var2–4*. Using a modified blue-native PAGE system, we reveal abnormal accumulations of photosystem I, photosystem II, and light-harvesting antenna complexes in *EVR3*/*EGY1*/*AMOS1* mutants. Moreover, we discover distinct roles of VAR2 and EVR3/EGY1/AMOS1 in the turnover of photosystem II reaction center under high light stress. In summary, our findings indicate that two chloroplast metalloproteases, VAR2/AtFtsH2 and EVR3/EGY1/AMOS1, function coordinately to regulate chloroplast development and reveal new roles of EVR3/EGY1/AMOS1 in regulating chloroplast proteostasis in Arabidopsis.

Chloroplasts are semi-autonomous organelles that originated from ancient prokaryotic cyanobacteria through endosymbiosis (1). During endosymbiosis, the majority of chloroplast genes were transferred to the nuclear genome, giving rise to contemporary chloroplast genomes with only ~100 protein-coding genes (2). The separation of genetic information responsible for the ~3000 chloroplast-localized proteins necessitates that proteins encoded by the nuclear genome must be synthesized in the cytosol, imported into chloroplasts, and assembled with chloroplast genome-encoded subunits to form functional multi-subunit photosynthetic complexes, such as photosystem II (PSII)[3] and photosystem I (PSI) (3). The coordinated expression of the two genomes is regulated at multiple levels, including transcriptional, translational, and posttranslational levels, to maintain the proper stoichiometry between protein subunits encoded by the two genomes (4, 5). The proteome of chloroplasts is also strikingly dynamic in response to diverse developmental signals and environmental cues (6). Genetic dissections of chloroplast development using leaf coloration as the phenotypic readout have been proven to be extremely fruitful as a spectrum of leaf color mutants ranging from albino, yellow, pale green, virescent, and variegation can be readily identified in genetic screens (7). These mutants serve as splendid genetic resources in elucidating the regulation of chloroplast development by nuclear-encoded chloroplast proteins. However, how these factors coordinate genetically to regulate chloroplast development remains largely unexplored.

Mutations in chloroplast proteases often result in arrested or delayed chloroplast development, highlighting the importance of proteostasis in chloroplasts (8, 9). One of the most intriguing chloroplast proteolytic systems is the thylakoid FtsH complex because of the unique leaf variegation phenotype of Arabidopsis *yellow variegated2* (*var2*) and *var1* mutants, defective in thylakoid FtsH complex components VAR2/AtFtsH2 and VAR1/AtFtsH5, respectively (10, 11). In Arabidopsis, thylakoid FtsH complexes are heterohexamers comprised of both type A (AtFtsH1 and VAR1/AtFtsH5) and type B (VAR2/AtFtsH2 and AtFtsH8) subunits, based on their functional redundancy and interchangeability (12, 13). In photosynthetic organisms, thylakoid FtsH complexes take part in the PSII repair cycle, particularly the turnover process of D1, the reaction center subunit of PSII (14–18). The absence of thylakoid FtsH complexes and Deg protease in Arabidopsis leads to inefficient degradation of D1 protein under photoinhibition conditions induced by high light (19–21). Moreover, thylakoid FtsH complexes are also essential for chloroplast development as the complete loss of either type A or type B FtsH subunits cause lethality (12, 13). In addition, the presence of undifferentiated plastids in white sec-

This work was supported by National Natural Science Foundation of China Grants 31741010 (to Y. Q.), 31770205 (to X. L.), and 31870268 (to F. Y.) and by Fundamental Research Funds for the Central Universities 2452018152 (to Y. Q.). The authors declare that they have no conflicts of interest with the contents of this article.

This article contains Figs. S1–S7 and Tables S1 and S2.

[1] These authors contributed equally to this work.

[2] To whom correspondence should be addressed: 22 Xinong Rd., Yangling, Shaanxi 712100, China. Tel. (Fax): 86-29-87091935; E-mail: xiayanliu@gmail.com.

[3] The abbreviations used are: PSII, photosystem II; PSI, photosystem I; BN, blue-native.

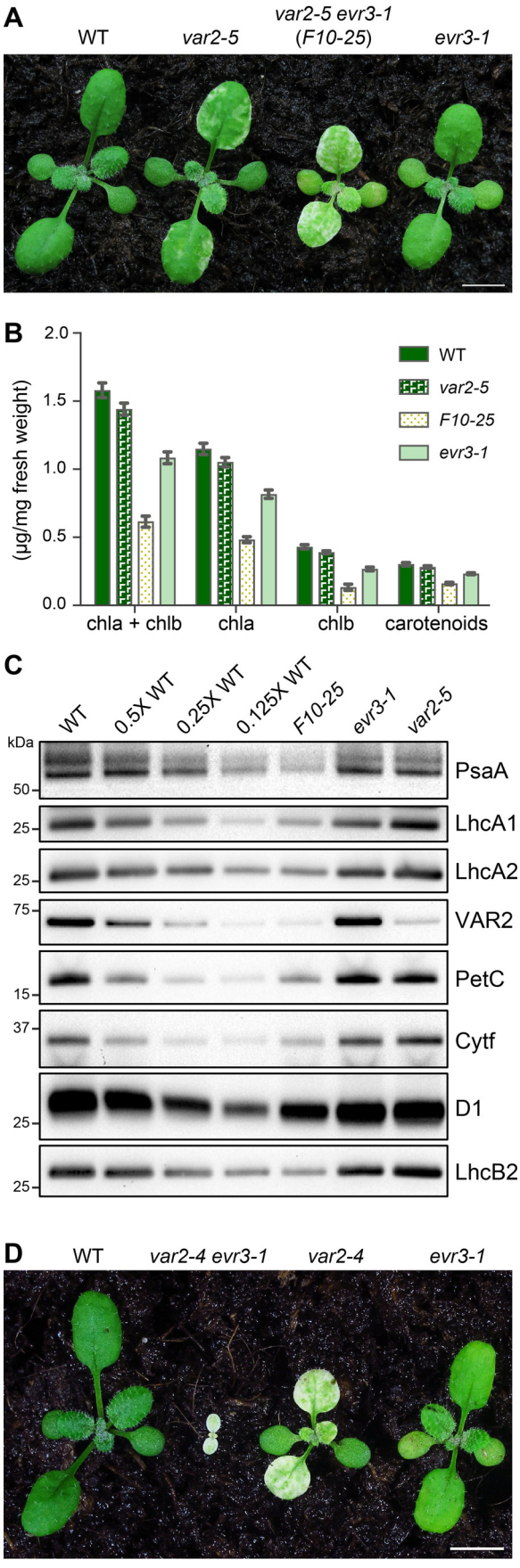

Figure 1. The enhancement of *var2* by *evr3–1*. *A*, phenotypes of representative 2-week-old WT, *var2–5*, *var2–5 evr3–1* (*F10–25*), and *evr3–1* plants. *Bar*, 5 mm. *B*, chlorophyll and carotenoid content of 2-week-old WT, *var2–5*, *var2–5 evr3–1* (*F10–25*), and *evr3–1*. Data were mean ± S.D. from three biological repeats. *C*, accumulation of representative thylakoid proteins in WT, *F10–25*, *evr3–1*, and *var2–5*. Total proteins were extracted from the first pair of true leaves of 2-week-old plants, and normalized to tissue fresh weight. Antibodies against PsaA, LhcA1, LhcA2, VAR2, PetC, Cytf, D1, and LhcB2 were used in immunoblots. *D*, phenotypes of representative 2-week-old WT, *var2–4 evr3–1*, *var2–4*, and *evr3–1* plants. *Bar*, 5 mm.

tors in *var2* also suggests that thylakoid FtsH complexes are involved in thylakoid biogenesis and chloroplast development (22).

To dissect the genetic mechanisms underlying leaf variegation and the regulation of chloroplast development, several research groups have taken advantage of the *var2* leaf variegation phenotype and isolated an increasing number of *var2* genetic suppressors, which reverse the white sector and variegation phenotype of *var2* mutants via extragenic mutations (23–27). We have identified the *SUPPRESSORS OF VARIEGATION* (*SVRs*) loci, which encode many components involved in chloroplast translation and gene expression (24, 28–34). The disruptions of these *SVR* genes cause a reduction in plastid gene expression and translation and are sufficient for the suppression of variegation phenotypes, thus establishing strong genetic and functional relationships between thylakoid FtsH complexes and plastid gene expression. The identification of a large number of *var2* genetic suppressor loci is consistent with the essential nature of thylakoid FtsH complexes, and indicates that *VAR2*/*AtFtsH2* may represent a highly connected genetic network hub (35).

To further explore the functional interaction network of *VAR2*/*AtFtsH2*, we systematically screened for *var2* genetic enhancer loci, termed *ENHANCERS OF VARIEGATION* (*EVRs*). Recently, we showed that mutations in *EVR1*/*RPS21b*, which encodes a cytosolic 40S ribosomal protein RPS21, and reduced activities of cytosolic translation enhance *var2* leaf variegation, revealing that the balance between cytosolic and chloroplast translation regulates VAR2-mediated chloroplast development (36). Here we report the identification of a new *EVR* locus, *EVR3*. Molecular cloning and complementation confirmed that loss-of-function mutations in *EVR3* greatly enhance *var2* leaf variegation, and *EVR3* encodes a chloroplast metalloprotease which was previously reported as ethylene-dependent gravitropism-deficient and yellow-green1 (EGY1) and ammonium overly sensitive1 (AMOS1) (37, 38). In addition, we uncovered previously unknown defects in PSI and PSII supercomplex assembly in *evr3*/*egy1*/*amos1* mutants. Moreover, we discovered that the PSII stability, particularly D1 stability, under high light is significantly compromised in *evr3–1* and further worsened in *var2–5 evr3–1* double mutant. Our findings establish that VAR2/AtFtsH2 and EVR3/EGY1/AMOS1 coordinate to regulate PSII stability and chloroplast development.

Results

Isolation of a var2–5 genetic enhancer mutant, evr3–1

To unravel the genetic regulatory network of chloroplast development, we took advantage of the leaf variegation phenotype of the *var2* mutant and systematically isolated *var2* extra-

genic enhancer loci, termed *EVRs* (36). Here we report the isolation of a new *var2–5* enhancer line, designated *F10-25* (Fig. 1*A* and Fig. S1*A*). We named this enhancer locus *EVR3*, and the original *F10-25* line represents *var2–5 evr3–1* double mutant. Although the *evr3–1* single mutant showed pale green leaf coloration and moderately reduced chlorophyll content compared with the WT, *F10–25* (*var2–5 evr3–1*) showed increased leaf variegation compared with *var2–5* and much lowered chlorophyll level compared with either of the parental single mutants (Fig. 1, *A* and *B*).

Next, we compared the steady state levels of chloroplast proteins representing key photosynthetic complexes in WT, *F10–25*, *evr3–1*, and *var2–5*. In accordance with the decrease in chlorophyll content, the accumulation of all major photosynthetic complexes we checked, including PSII (represented by D1), PSI (represented by PsaA), PSI and PSII antenna (represented by LhcA1, LhcA2 and LhcB2), and cytochrome b_6f (represented by Cytf and PetC), were dramatically reduced in *F10–25* compared to either *evr3–1* or *var2–5* (Fig. 1*C*). Consistent with the notion of *var2–5* being a leaky allele, reduced VAR2 accumulation was detected *var2–5* (Fig. 1*C*) (10). However, VAR2 level was comparable in WT and *evr3–1* (Fig. 1*C*), indicating that the enhancement of *var2–5* by *evr3–1* was not through direct impairment of FtsH complex accumulation.

Finally, we tested the genetic interaction between *evr3–1* and *var2–4*, a likely null allele of *var2* (10, 12). Interestingly, we identified albino plants that have the *var2–4 evr3–1* genotype in the F2 progeny of a cross between *evr3–1* and *var2–4*, but these seedlings do not survive the cotyledon stage (Fig. 1*D*). Albino plants segregated from the same F2 progeny grown on sucrose-containing medium could develop a few true leaves but were not autotrophic (Fig. S1*B*). PCR-based genotyping confirmed that these white seedlings were *var2–4 evr3–1* double mutants (Fig. S1*C*). The synthetic lethality observed in *var2–4 evr3–1* double mutant, indicated that *VAR2* and *EVR3* act synergistically to promote chloroplast development and together *VAR2* and *EVR3* gene activities are essential for establishing phototrophic growth under our growth conditions.

EVR3 is EGY1/AMOS1

To uncover the molecular lesion in *evr3–1*, a whole genome resequencing strategy was adopted using pooled genomic DNAs of *evr3–1* seedlings from a segregating F2 population of a backcross between *evr3–1* and WT. A G to A point mutation that would cause a Gly432Glu missense mutation in the protein coded by *At5g35220* was identified in *evr3–1* (Fig. 2, *A* and *B*). *At5g35220* was previously reported as *EGY1/AMOS1*, encoding a chloroplast thylakoid membrane-localized S2P-like metalloprotease (37, 38). EGY1/AMOS1 contains a conserved zinc-binding motif HE*XX*H localized between putative TM2 and TM3, and a NPDG motif localized between putative TM6 and TM7 (Fig. S1, *D* and *E*) (39). These two motifs are required for the proteolytic activity of S2P in animals and S2P-like homologues in plants (40). Evolutionarily, EGY1/AMOS1 homologues are present in most photosynthetic organisms (Fig. S1, *D* and *E*). The mutated Gly^{432} in *evr3–1* is conserved in photosynthetic organisms and is localized next to the NPDG motif (Fig. S1*E*).

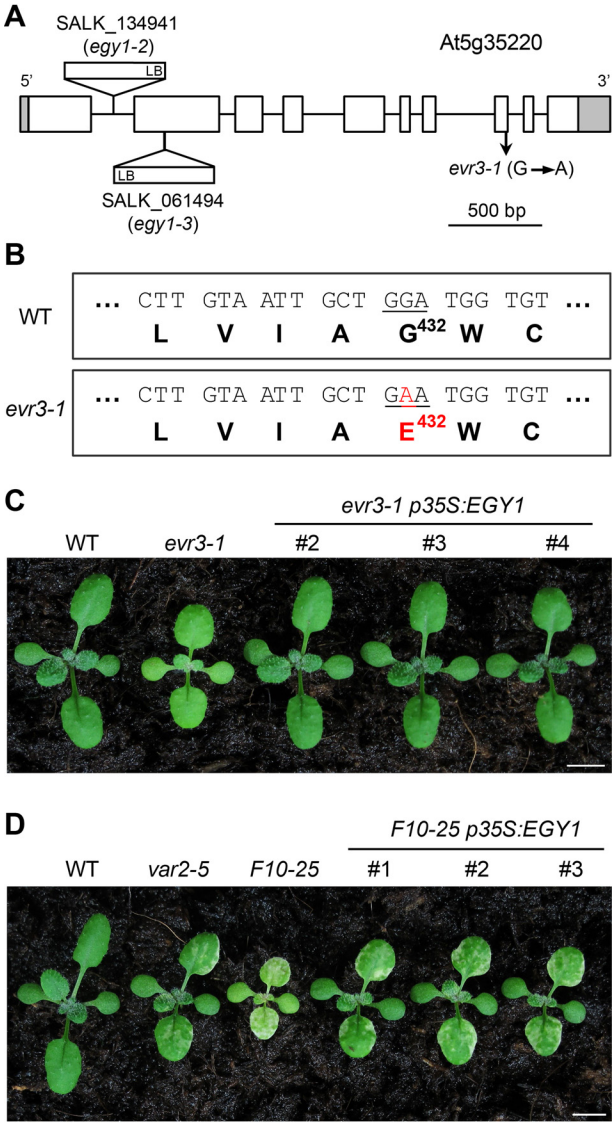

Figure 2. Identification of the *EVR3* locus. *A*, schematic representation of the mutation sites in *evr3–1* and two T-DNA insertion lines, *egy1–2* and *egy1–3* in the At5g35220 gene model. Introns and exons were represented by *solid lines* and *boxes*, respectively. *Shaded boxes* indicated 5′ and 3′ untranslated regions. *B*, the G432E mutation identified in *evr3–1*. *C*, phenotypes of representative 2-week-old WT, *evr3–1*, and three independent complementation lines expressing *p35S:EGY1* in *evr3–1* background. *Bar*, 5 mm. *D*, phenotypes of representative 2-week-old WT, *var2–5*, *evr3–1*, and three independent complementation lines expressing *p35S:EGY1* in *F10–25* background. *Bar*, 5 mm.

Phenotypically, the pale green leaf color of *evr3–1* resembled the two reported T-DNA mutant alleles of *EGY1/AMOS1*, *egy1–2* (SALK_134931), and *egy1–3* (SALK_061494) (Fig. 2*A* and Fig. S2*A*) (37). In addition, *evr3–1* cannot complement *egy1–2* as F1 progeny of a cross between *evr3–1* and *egy1–2* showed pale green leaf phenotype similar to *evr3–1* and *egy1–2* but not WT (Fig. S2*A*). Similar to *evr3–1*, *egy1–2* and *egy1–3* could also enhance *var2* leaf variegation (Fig. S2, *B–G*). These observations suggest that *evr3–1* is a new mutant allele of *EGY1/AMOS1*.

More importantly, expression of WT *EGY1/AMOS1* under the control of the Cauliflower Mosaic Virus 35S promoter promoter (*p35S:EGY1*) in *evr3–1* single mutant yielded multiple

transgenic lines resembling WT (Fig. 2*C* and Fig. S3*A*). Next, we tested whether the same *p35S:EGY1* could also complement *F10–25*. Because of the greatly reduced fertility of *F10–25*, we transformed *p35S:EGY1* into plants that were *var2–5* heterozygous and *evr3–1* homozygous (*var2–5*/+ *evr3–1*). At T2 generation, multiple transgenic lines expressing *p35S:EGY1* that were *var2–5 evr3–1* double homozygous but display a leaf variegation phenotype similar to that of *var2–5* were identified (Fig. 2*D* and Fig. S3*B*). These data provide conclusive proof that *EVR3* is *EGY1/AMOS1*, and that the disruption of *EVR3/EGY1/AMOS1* enhances *var2–5* leaf variegation.

EVR3/EGY1/AMOS1 is required for the accumulation of antenna proteins during de-etiolation

As a chloroplast protease, EGY1 is expected to have a role in chloroplast proteostasis (37). We noticed that the abundance of antenna proteins, such as LhcA1, LhcA2, and LhcB2 was reduced in *evr3–1* (Fig. 1*C*). This is in agreement with previous report that the disruption of *EGY1* leads to significantly decreased levels of LHCI and LHCII antenna proteins (37, 41). In contrast, steady state levels of FtsH or cytochrome b_6f complex subunits were unaffected in *evr3–1* compared with those in the WT (Fig. 1*C*). These observations suggest a specific role of EVR3/EGY1/AMOS1 on the accumulation of antenna proteins. To test if EGY1/AMOS1 is involved in the accumulation of antenna proteins, we utilized a de-etiolation system, which could provide a clear starting time point for the accumulation of photosynthetic proteins. Etiolated seedlings were transferred to light, and the amount of photosynthetic proteins was monitored and quantified during greening. We found that the rate and extent of increase in most photosynthetic subunits, including nuclear genome-encoded subunits such as PetC, RbcS, and VAR2, and also plastid genome-encoded subunits such as D1 and Cytf were similar in WT and *evr3–1* during de-etiolation (Fig. 3, *A* and *B*). In contrast, LHCI and LHCII antenna proteins, such as LhcA2 and LhcB2, were readily detectable in WT but remained undetectable in *evr3–1* after transfer to light for 3 h. 6 h after transfer to light, high levels of antenna proteins accumulated in WT whereas greatly reduced amounts of LhcA2 and LhcB2 were detected in *evr3–1* (Fig. 3, *A* and *B*). These data uncover a critical role of EGY1 for the efficient accumulation of antenna proteins in response to light, a process critical for germinating seedlings to establish photosynthesis and autotrophic growth.

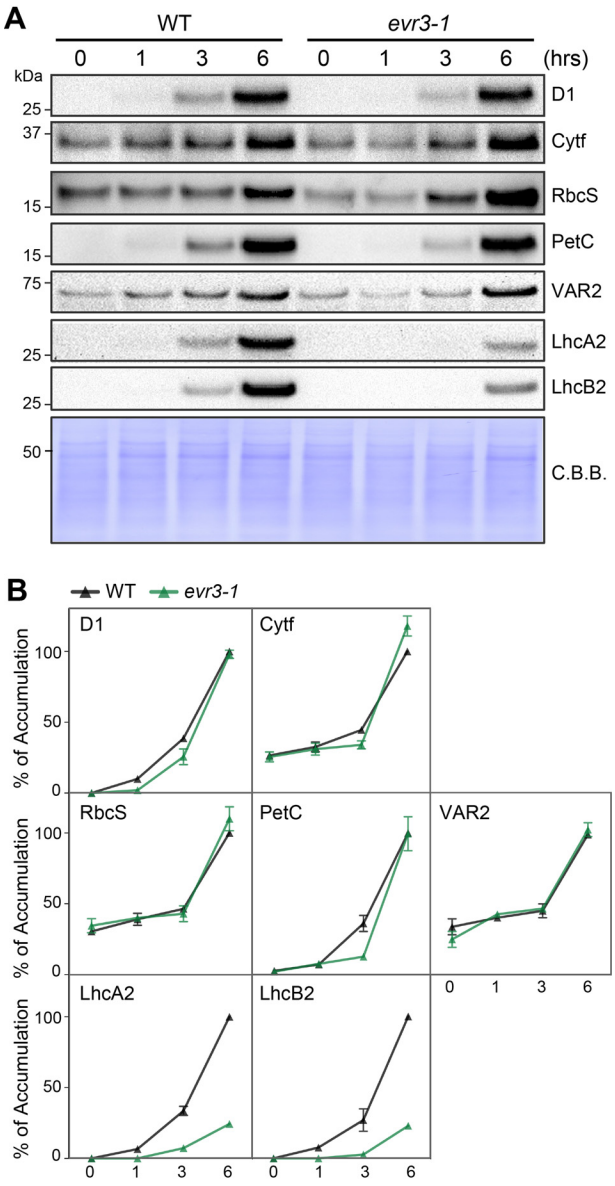

Figure 3. Time-course analysis of thylakoid proteins accumulations in WT and *evr3–1* during de-etiolation. *A*, immunoblotting analysis of thylakoid proteins in etiolated WT and *evr3–1* seedlings that were transferred to light for 0, 1, 3, and 6 h. Loadings are normalized by tissue fresh tissue weight. Antibodies against D1, Cytf, RbcS, PetC, VAR2, LhcA2, and LhcB2 were used. Coomassie Brilliant Blue (*C. B. B.*)–stained PVDF membrane served as the loading control. *B*, quantification of immunoblots shown in *A*. The relative protein level was determined based on signal intensities of protein bands. In each blot, signal intensity of the protein band from the 6-h light-treated WT seedling was defined as 100%. Data were presented as mean ± S.D. of three blots obtained from independent biological replicates.

Loss of EVR3/EGY1/AMOS1 leads to abnormal accumulation of photosystem I complexes

To explore the role of *EVR3/EGY1/AMOS1* in chloroplast proteostasis, we probed the status of thylakoid photosynthetic complexes in WT and *evr3–1* using blue-native PAGE (BN-PAGE). First, we utilized the classic *n*-dodecyl-β-D-maltoside solubilization method and observed a conspicuous reduction of LHCII antenna trimers in *evr3–1* (Fig. S4). Next, we employed a BN-PAGE solubilization method based on nonionic detergent digitonin, which can reveal additional protein complex information (42). Surprisingly, in addition to the reduced level of LHCII antenna trimers in *evr3–1*, the banding pattern of thylakoid photosynthetic complexes was clearly altered in *evr3–1* compared with WT, with the most pronounced differences in the region of the 1-D BN-PAGE gel where three major PSI complexes, B1, B2, and B3, were found (Fig. 4*A*) (42). B1, B2, and B3 correspond to PSI-LHCI-LHCII, PSI-LHCI, and PSI core, respectively (42). 1-D BN-PAGE showed that B1 was markedly reduced, B2 remained unchanged, and B3 was overaccumulated in *evr3–1* compared with those in the WT (Fig. 4, *A* and *B*). Identities of B1, B2, and B3 complexes were validated by immunoblot analyses of proteins extracted from their native gel bands using antibodies against PSI core subunits and antenna proteins (Fig. 4*C*). We detected PSI core subunits

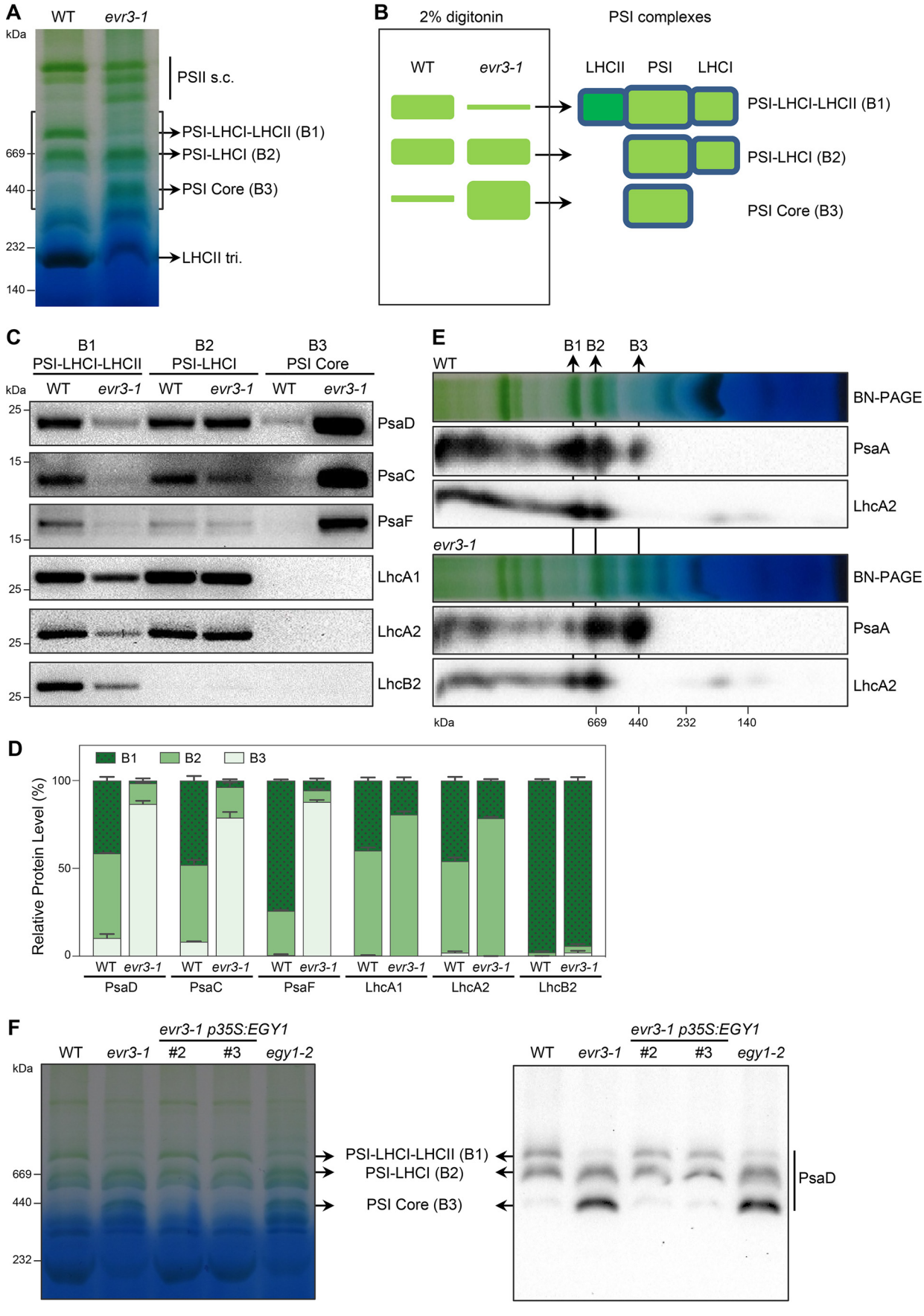
A
WT
evr3-1
kDa
669
440
232
140
PSII s.c.
PSI-LHCI-LHCII (B1)
PSI-LHCI (B2)
PSI Core (B3)
LHCII tri.
B
2% digitonin
PSI complexes
WT
evr3-1
LHCII
PSI
LHCI
PSI-LHCI-LHCII (B1)
PSI-LHCI (B2)
PSI Core (B3)
C
B1
PSI-LHCI-LHCII
B2
PSI-LHCI
B3
PSI Core
kDa
WT
evr3-1
PsaD
PsaC
PsaF
LhcA1
LhcA2
LhcB2
E
WT
B1 B2
B3
BN-PAGE
PsaA
LhcA2
evr3-1
kDa
669
440
232
140
D
B1
B2
B3
Relative Protein Level (%)
100
50
0
PsaD
PsaC
PsaF
LhcA1
LhcA2
LhcB2
F
evr3-1 p35S:EGY1
WT
evr3-1
#2
#3
egy1-2
kDa
669
440
232
PSI-LHCI-LHCII (B1)
PSI-LHCI (B2)
PSI Core (B3)
PsaD

(PsaD, PsaC, and PsaF), LhcAs and LhcB2 in B1 complexes, and these proteins were less abundant in *evr3–1* (Fig. 4, *C* and *D*). LhcB2 is absent in B2 complexes, consistent with its PSI-LHCI identity (Fig. 4, *C* and *D*). Overall accumulations of PSI core and LHCI proteins in B2 complexes were similar in WT and *evr3–1* (Fig. 4, *C* and *D*). In the B3 complex, we observed markedly increased levels of PSI core subunits in *evr3–1*, in contrast to their low presence in WT (Fig. 4, *C* and *D*). Finally, to gain a more comprehensive picture of proteins in B1, B2, and B3 complexes, 2-D BN/SDS-PAGEs were performed. Immunoblots of the 2-D gels confirmed that PSI-LHCI-LHCII, *i.e.* the B1 complex, was reduced in *evr3–1*, although PSI core, *i.e.* the B3 complex, was more abundant in *evr3–1* (Fig. 4*E*).

Importantly, the abnormal PSI complexes observed in *evr3–1* were reversed to patterns similar to WT in complementation lines (Fig. 4*F*). Similar PSI defects were also observed in two other *egy1* alleles, *egy1–2* and *egy1–3* (Fig. S5*A*). These findings indicate that the abnormal accumulation of PSI complexes in *evr3–1* is a direct consequence of the lack of functional EVR3/EGY1/AMOS1. Together, these results establish that EVR3/EGY1/AMOS1 is required for the proper accumulation of PSI complexes.

Loss of EVR3/EGY1/AMOS1 leads to more photosystem II dimer and monomer accumulation

Using the digitonin solubilization BN-PAGE procedure, we next examined the status of various PSII complexes in WT, *var2*, and *evr3–1*. We observed no conspicuous differences in major PSII complexes between WT and *var2* mutants, including both *var2–4* and *var2–5* (Fig. S6). This observation was further confirmed by silver staining of the 2-D BN/SDS-PAGE gels (Fig. S7). However, we noticed that migration patterns of CP47-containing PSII complexes were not identical in WT and *evr3–1* in silver-stained 2-D BN/SDS-PAGE gels (Fig. S7), suggesting abnormalities in the accumulation of PSII complexes in *evr3–1*. To explore the abnormalities of PSII complex accumulation in *evr3–1*, we performed immunoblotting of BN-PAGE with antibodies against PSII core subunits D2 and CP47, and LHCII subunit LhcB2. We found that although the amount of PSII monomer LHC trimer complex was similar in WT and *evr3–1*, PSII dimer and PSII monomer were dramatically overaccumulated in *evr3–1* compared with those in the WT (Fig. 5, *A–C*). Similar PSII defects were also found in *egy1–2* and *egy1–3* (Fig. S5*B*). These data revealed that EVR3/EGY1/AMOS1 is required for the homeostasis of PSII complexes.

VAR2/AtFtsH2 and EVR3/EGY1/AMOS1 regulate PSII stability under high light

Previously, VAR2/AtFtsH2 has been shown to be involved in the repair cycle of PSII subunits, particularly D1 degradation under high light conditions (14–16). Given the synergistic interaction between *evr3–1* and *var2*, as well as the abnormal accumulations of PSI and PSII complexes in *evr3–1*, we reasoned that VAR2/AtFtsH2 and EVR3/EGY1/AMOS1 may both function in the PSII repair cycle to control the stability of PSII subunits under high light stress. To monitor the stability of major photosynthetic proteins under high light stress, WT and mutant leaf discs were infiltrated with lincomycin and cycloheximide to block both chloroplast and cytosol translation during high light treatment. After 0-, 2-, and 4-hour high light treatment, levels of representative subunits of major photosynthetic complexes, including PSII (D1, D2, CP47, and CP43), PSI (PsaD and PsaF), LHCI (LhcA1 and LhcA2), LHCII (LhcB2), and cytochrome b_6f (Cytf), were analyzed with immunoblotting. Cytf, which has been reported to remain stable under high light stress, was included as a control to normalize the loading of immunoblots (43).

Upon high light treatment, although with varied rates, gradual degradations of PSII core subunits (D1, D2, CP47, and CP43) were observed in WT, *var2–5*, *evr3–1*, and *var2–5 evr3–1* double mutant, whereas PSI subunits remained stable in all the genotypes during our highlight treatment (Fig. 6, *A* and *B*). In *var2–5*, the degradation of PSII reaction center proteins D1 and D2 was partially blocked compared with WT (Fig. 6, *A* and *B*). These observations are consistent with previous reports (15, 16). Degradations of all four PSII core subunits examined were faster in *evr3–1* than in WT (Fig. 6, *A* and *B*). In addition, antenna proteins, especially LHCI subunits, were less stable in *evr3–1* compared with those in WT (Fig. 6, *A* and *B*). Interestingly, in *var2–5 evr3–1* double mutants, D1 and D2 become less stable with degradation rates similar to those of *evr3–1*, indicating the blockage of D1 and D2 degradation caused by the *var2–5* mutation was bypassed by the loss of *EVR3/EGY1/AMOS1* (Fig. 6, *A* and *B*). Our findings indicate that although VAR2 is necessary for the turnover of D1 and D2, EVR3/EGY1/AMOS1 is required for stabilizing PSII core proteins. PSII repair cycle probably needs coordinated actions of VAR2/AtFtsH2 and EVR3/EGY1/AMOS1 under high light stress.

Discussion

Single gene–based molecular genetic analysis has served as the cornerstone of modern molecular biology. However, comprehensive genetic interactions and networks have to be established to tackle the genotype to phenotype, and ultimately, the genome to phenome question. The fascinating leaf variegation phenotype of the *var2* mutant has long attracted geneticists' interest and enables genetic screens for both genetic suppressor and enhancers (23–27, 36). Enhancer screens are powerful tools to reveal close functional relationships (44). In the case of

Figure 4. Abnormal accumulation of PSI complexes in *evr3–1*. *A*, thylakoid membranes from 4-week-old WT and *evr3–1* were solubilized with digitonin and resolved by BN-PAGE. The *gray box* indicated the region containing PSI complexes such as PSI-LHCI-LHCII (B1), PSI-LHCI (B2), and PSI Core (B3). *LHCII tri.*, LHCII trimer; *PSII s.c.*, PSII supercomplexes. *B*, schematic depiction of the PSI complexes accumulation defects in *evr3–1* shown in *A*. *C*, the B1, B2, and B3 complexes from *A* were cut in gel and re-solubilized with 2× SDS sample buffer for immunoblotting. Antibodies against PsaD, PsaC, PsaF, LhcA1, LhcA2, and LhcB2 were used. *D*, quantifications of immunoblots shown in *C*. Relative distributions of indicated subunits in B1, B2, and B3 complexes were shown in *stacked bar graphs*. For each protein subunit analyzed, total signal intensities of protein bands found in B1, B2, and B3 complexes are defined as 100%. Data were presented as mean ± S.D. of three blots obtained from independent biological replicates. *E*, BN-PAGE gel lanes shown in *A* were cut and resolved by SDS-PAGE. Antibodies against PsaA and LhcA2 were used in immunoblotting after 2-D BN/SDS-PAGE. *F*, the accumulations of PSI complexes were examined in WT, *evr3–1*, two *evr3–1 p35S:EVR1* complementation lines, and *egy1–2*. BN-PAGE was performed as in *A*. 1-D BN-PAGE gel was blotted directly with the PsaD antibody to detect PSI complexes.

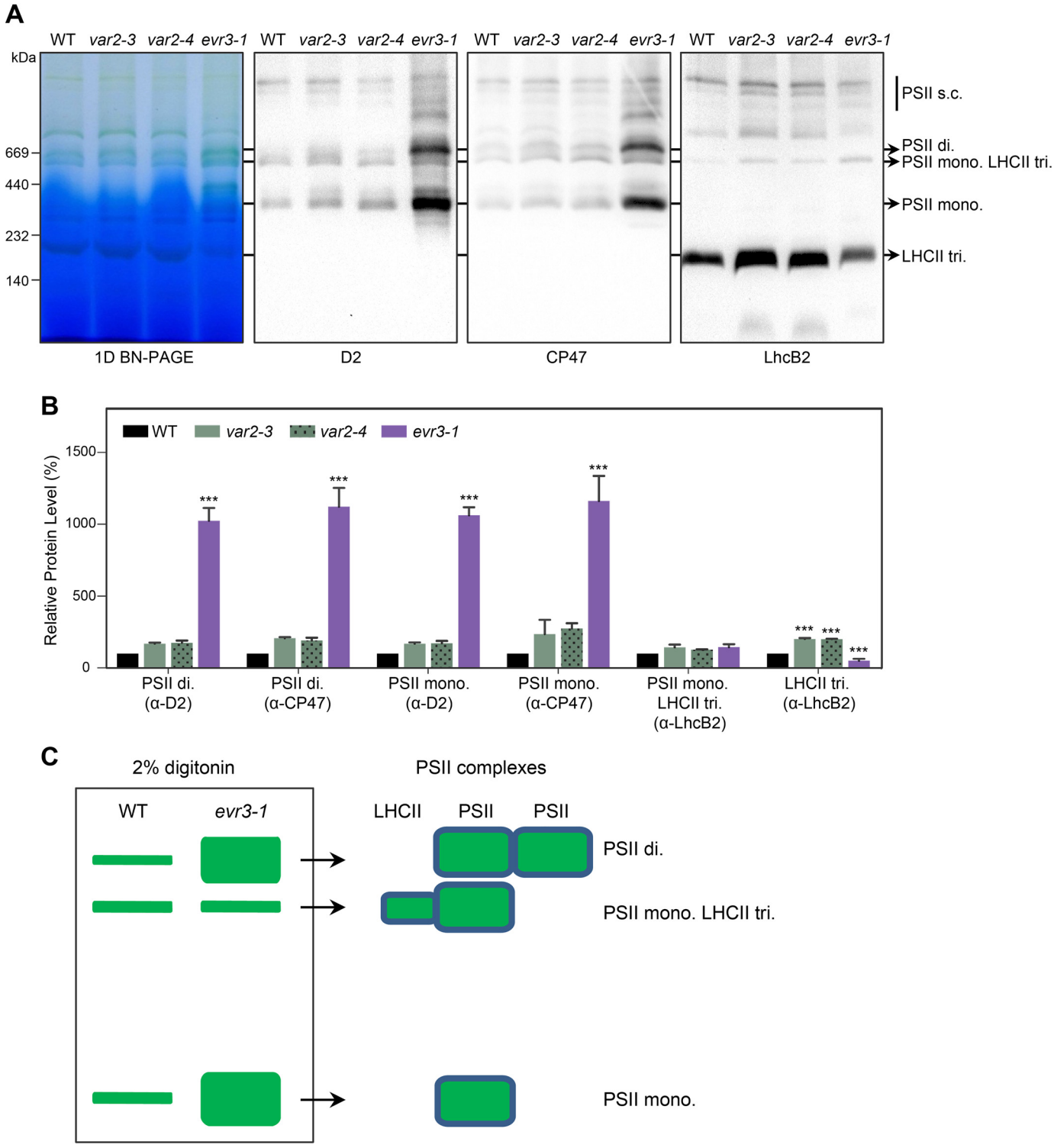

Figure 5. Abnormal accumulation of PSII complexes in *evr3–1*. *A*, thylakoid membranes from 4-week-old WT, *var2–3*, *var2–4*, and *evr3–1* were solubilized with 2% digitonin, resolved by BN-PAGE, and probed with antibodies against D2, CP47, and LhcB2. Positions of different PSII complexes were marked by *arrows*. *PSII s.c.*, PSII supercomplex; *PSII di*, PSII dimer; *PSII mono*, PSII monomer; *PSII mono LHCII tri*, monomeric PSII core with LHCII trimer. *B*, quantifications of immunoblots shown in *A*. In each blot, signal intensity of the indicated protein band from the WT sample was defined as 100%. Data were presented as mean ± S.D. of three blots obtained from independent biological replicates. ***, $p < 0.001$; one-way analysis of variance (ANOVA) followed by Dunnett's multiple comparisons test (WT *versus* mutant). *C*, schematic depiction of the PSII complexes accumulation defects in *evr3–1* shown in A.

VAR2/*AtFtsH2*, it is known that enhancement of chloroplast development defects can be generated by combining *var2* mutations with mutations in FtsH subunit genes *VAR1*/*AtFtsH5* and *AtFtsH8* (12, 13). In this work, we isolated a new *var2* enhancer locus, *EVR3*. We confirmed that *EVR3* is identical to the previously reported locus *EGY1*/*AMOS1* (37, 38). Initially identified based on pigmentation-deficient and defective in ethylene-stimulated gravitropic responses, *EVR3*/*EGY1*/

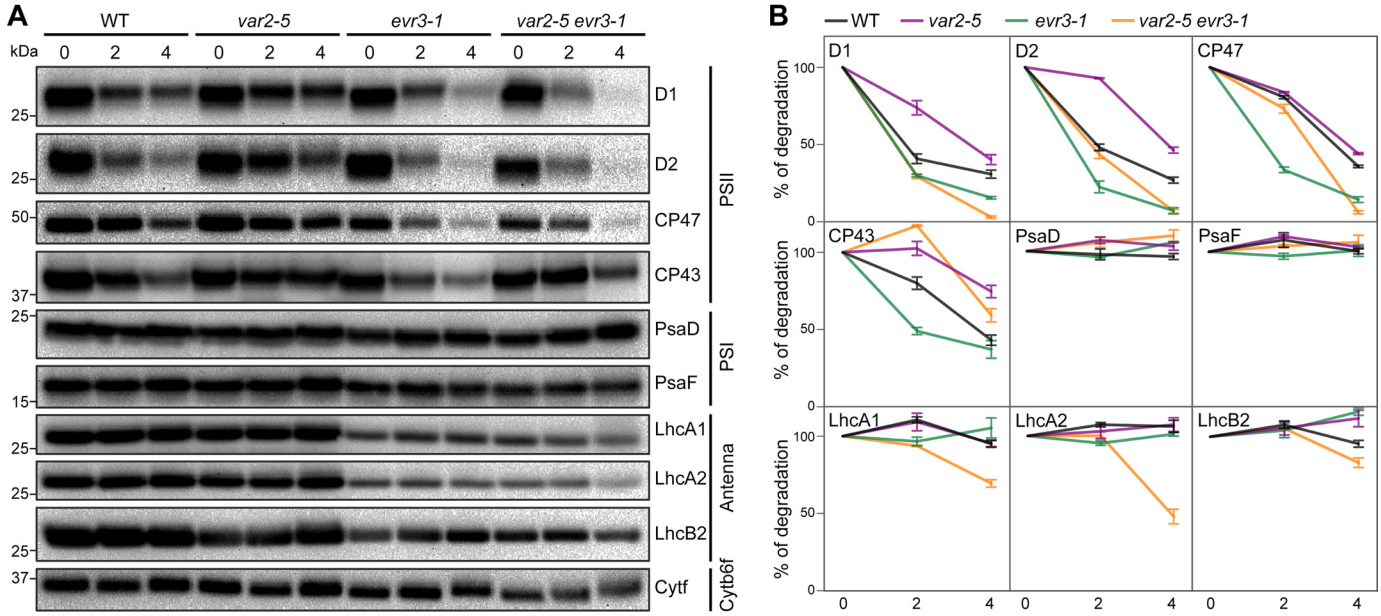

Figure 6. Stability of photosynthetic complexes in WT, *var2–5*, *evr3–1*, and *var2–5 evr3–1* under high light. *A*, leaf discs from the seventh or eighth true leaves of 4-week-old plants infiltrated with translation inhibitors lincomycin and cycloheximide were treated with high light (~1000 μmol m^{-2} s^{-1}). Amounts of photosynthetic proteins after 0-, 2- and 4-hour high light treatment were analyzed with immunoblots. Antibodies against D1, D2, CP47, and CP43 for PSII, PsaD, and PsaF for PSI, LhcA1, LhcA2, and LhcB2 for antenna complexes, Cytf for cytochrome b_6f complex were used. *B*, quantifications of immunoblots shown in *A*. In each blot, protein band signal intensity at 0 h high light treatment was defined as 100% for each genotype. Loadings were normalized to the levels of Cytf. Data were presented as mean ± S.D. of three blots obtained from independent biological replicates.

AMOS1 encodes a chloroplast membrane-bound ATP-independent metalloprotease (37, 41). Loss of *EVR3/EGY1/AMOS1* causes similar chloroplast impairment in Arabidopsis, tomato (*Solanum lycopersicum*), and monocot foxtail millet (*Setaria italica*), suggesting a conserved role of EGY1 homologs (45, 46). In addition to chloroplast development and ethylene signaling, *EVR3/EGY1/AMOS1* also regulates plant tolerance to ammonium toxicity through the abscisic acid signaling pathway (38). Loss of *EVR3/EGY1/AMOS1* also confers resistance to phosphate starvation via modulating the relative levels of abscisic acid and ethylene in roots (47).

Our findings focus on the role of EGY1 in chloroplast. We show that the collective activities of EVR3/EGY1/AMOS1 and VAR2/AtFtsH2 are essential for chloroplast development in *Arabidopsis thaliana* (Fig. 1), thus establish a previously unknown functional connection between these two metalloproteases.

Chloroplast thylakoid membrane protein complexes, including PSII, PSI, cytochrome b_6f, and ATP synthase, catalyze the critical conversion of light energy to chemical energy (48). More importantly, photosynthetic protein complex assemblies are under dynamic regulation by numerous factors, responding to developmental and environmental inputs. For example, to optimize light energy harvest, LHCII trimers, the major light harvesting complexes of PSII, can disassociate from PSII and instead bind to PSI to balance the energy inputs between PSII and PSI, thus constituting the state transition regulation (49). Native gel electrophoresis analysis has been successfully used to probe the status of membrane protein complexes and a modified native gel system based on the mild detergent digitonin has been shown to reveal additional photosynthetic protein complex information (42). Using this system, our detailed native gel analyses revealed previously unreported PSI and PSII assembly defects in *evr3*/*egy1* mutants (Figs. 4 and 5). First, we discovered that the accumulation of PSI-LHCI-LHCII (B1) complex was dramatically reduced in *evr3–1* mutants (Fig. 4). This suggests that EGY1 is required for the association of LHCII with PSI under our growth conditions. Concurrent with this, the level of LHCII trimers were also greatly reduced in *evr3–1* mutants, potentially leading to reduced availability of LHCII trimers for PSI. The abnormal accumulation of PSI core (B3) complex is puzzling, suggesting that EGY1 may also be necessary for the binding of LHCI to the PSI core complex to form PSI-LHCI (B2) complex (Fig. 4). In addition, PSII assembly is also perturbed in *evr3–1* mutants and we discovered abnormal accumulations of PSII dimer and PSII monomer in *evr3–1* mutants (Fig. 5). It is interestingly to note that the over-accumulation of these PSII complexes is accompanied also by the reduction of LHCII trimers (Fig. 5). The reduction of LHCII trimers is consistent with reported abnormal accumulation of light harvesting proteins in *egy1* mutants (37). Although we lack direct cause and effect evidence, it is possible that the reduced LHCII trimers may trigger the PSI and PSII defects in *evr3–1* mutants.

One of the most intriguing regulations of photosynthetic protein complexes is the turnover process of PSII (18). The highly oxidative reactions of PSII put great stress on PSII components, particularly reaction center D1 protein, which is long known to undergo a rapid turnover process (50). Chloroplast FtsH and Deg proteases are intimately involved in the degradation of damaged D1 protein (19–21). Consistently, the degradation of D1 protein under high light conditions was slowed in *var2* mutants, indicating an involvement of VAR2/AtFtsH2 and thylakoid FtsH complexes in regulating D1 degradation (Fig. 6) (14–17). Surprisingly, we uncovered a previously unknown involvement of EVR3/EGY1/AMOS1 in the D1 turnover pro-

cess. Under high light conditions, the degradation of D1 was much faster in *evr3–1* mutants than in WT (Fig. 6). This finding is counterintuitive as the absence of a protease, EVR3/EGY1/AMOS1, leads to accelerated protein degradation, and suggests that D1 is not the direct substrate of EVR3/EGY1/AMOS1. Moreover, the slowed degradation of D1 in *var2* mutants was somehow bypassed by the mutation in *EVR3*/*EGY1*/*AMOS1* as *evr3–1 var2–5* has a D1 degradation rate similar to that of *evr3–1* (Fig. 6). These findings suggest the existence and/or activation of alternative protein degradation capacities in the absence of both VAR2/AtFtsH2 and EVR3/EGY1/AMOS1 to facilitate D1 degradation.

Despite the PSII and PSI assembly defects, mutants of *EVR3*/*EGY1*/*AMOS1* display pale green leaf coloration, rather than a leaf variegation phenotype. The synthetic lethal combination of *VAR2*/*AtFtsH2* and *EVR3*/*EGY1*/*AMOS1* mutations may stem from the abnormal assembly of PSII and PSI, or the aberrant D1 degradation, and eventually leading to an enhancement of *var2* leaf variegation phenotype. We have proposed a threshold hypothesis in which the reduced thylakoid FtsH complexes in *var2* mutants may generate a sensitized chloroplast state ideal for the identification of factors that act together with VAR2/AtFtsH2 to regulate chloroplast development (32). In the context of the threshold hypothesis, the defects caused by *EVR3*/*EGY1*/*AMOS1* mutations generate far more dramatic consequences in the more sensitized *var2* mutant backgrounds than the *EVR3*/*EGY1*/*AMOS1* mutation alone. Our genetic and biochemical evidence indicate that *VAR2*/*AtFtsH2* and EVR3/EGY1/AMOS1 act synergistically to regulate chloroplast development.

Experimental procedures

Plant materials and growth conditions

All Arabidopsis (*Arabidopsis thaliana*) lines used in this research are in the Columbia-0 ecotype background. *F10–25* (*var2–5 evr3–1*) was recovered in an ethyl methanesulfonate–induced mutant pool. *evr3–1* single mutant was obtained by backcrossing *F10–25* with WT to remove *var2–5*. The synthetic lethal double mutant *var2–4 evr3–1* was maintained by self-fertilization of *var2–4* homozygous *evr3–1* heterozygous lines (*var2–4 evr3–1*/+). *var2–3*, *var2–4*, and *var2–5* have been described (10, 12). Two T-DNA insertion *egy1* mutants, *egy1–2* (SALK_134931) and *egy1–3* (SALK_061494), have been described (37) and were obtained from the Arabidopsis Biological Resource Center. For general purposes, plants were grown on commercial soil mix (Pindstrup, Denmark) in a plant growth room (22 °C and continuous illumination of ~100 μmol m^{-2} s^{-1} light intensity). For de-etiolation assay, surface-sterilized seeds were grown on vertical plates containing 1/2 Murashige and Skoog medium (1/2 MS) and 1% Bacto Agar for 3 days in the dark at 22 °C before placing under light for indicated time periods. Point mutations of *var2–4*, *var2–5*, and *evr3–1* were genotyped by the Derived Cleaved Amplified Polymorphic Sequences method (51). Primers used in genotyping were listed in Table S1.

Quantification of chlorophyll content

Leaves of 2-week-old plants grown on soil mix were harvested, weighed, and ground in liquid nitrogen. 95% ethanol (v/v) was then added to extract chlorophyll pigments at 4 °C for 24 h in the dark. The content of chlorophylls and carotenoids was calculated as described in Ref. 36. Three biological replicates for each genotype were included.

Whole genome resequencing

evr3–1 was backcrossed with Col-0 for five times. In the F2 generation of the last round backcross, seedlings of 60 individuals with *evr3–1* phenotype were pooled together to extract DNA using the DNAquick Plant System kit (TIANGEN Biotech). *evr3–1* genomic DNA library preparation, genome resequencing, and sequencing data analysis were performed at Novogene. In brief, DNA sequencing library was prepared using the NEBNext® Ultra™ DNA Library Prep Kit for Illumina® (New England Biolabs) following the manual provided by the manufacturer. Library was assessed using the Agilent Bioanalyzer 2100 system before sequenced on an Illumina HiSeq4000 platform and 150 bp paired-end reads were generated. Filtered clean reads were aligned to the TAIR10 reference genome. Single nucleotide polymorphisms between the reference genome sequence and pooled F2 mutant DNA sequence were detected and annotated. We selected homozygous nonsynonymous G to A single nucleotide polymorphisms located in the gene regions as candidate mutations. The G to A mutation found in *EGY1*/*AMOS1*/At5g35220 was confirmed by conventional Sanger sequencing and was focused for further analysis because of the phenotypic resemblance of *evr3–1* with the reported *egy1* mutant alleles.

Transgenic lines

For complementation assay, the coding region of *EVR3*/At5g35220 was amplified from WT cDNA with primers AT5G35220 F and AT5G35220 R (Table S1). The PCR product was cloned into a modified binary vector *pBI111L-intron* to place the At5g35220 ORF under the control of 35S promoter (28). The resulting construct was sequenced and used to transform *evr3–1* single mutant and *var2–5* heterozygous *evr3–1* homozygous (*var2–5*/+ *evr3–1*) using the floral dip method (52). T1 transgenic lines were screened on 1/2 Murashige and Skoog plates with 50 mg $liter^{-1}$ kanamycin. Genotypes of the transgenic lines were confirmed by PCR using sequence-specific primers. Genotyping primers are listed in Table S1.

Total protein extraction and immunoblot analysis

Fresh plant materials were weighed, ground in liquid nitrogen, and extracted with 2× SDS sample buffer (0.125 M Tris-HCl, pH 6.8, 4% SDS, 20% glycerol, 2% β-mecaptoethanol, and 0.02% bromphenol blue) at 65 °C for 30 min. The volume of 2× SDS sample buffer was normalized based on sample fresh weight. For immunoblotting, total proteins were separated with 12% SDS-PAGE containing 8 M urea, transferred onto PVDF membranes (0.22 μm, Millipore), and probed with indicated antibodies. The source of antibodies used in this study is listed in Table S2. Representative immunoblots from three indepen-

dent biological replicates were shown. Quantification of immunoblots were carried out with the Image Lab software (Bio-Rad). Graphs were generated with the GraphPad Prism 8 software.

Preparation of thylakoid membranes, BN-PAGE, and silver staining

Preparation of thylakoid membranes and blue-native PAGE was performed as described (42), with some modifications in solubilizing thylakoid membranes. Briefly, for solubilization with β-dodecylmaltoside, thylakoids equivalent to equal amounts of total protein were solubilized with 25BTH20G buffer (25 mM BisTris-HCl, pH 7.0, 20% glycerol) containing 1% *n*-dodecyl-β-D-maltoside (w/v). For solubilization with digitonin, thylakoids equivalent to equal amounts of total protein were solubilized with 2% digitonin (w/v) in 25BTH20G buffer. For 1-D BN-PAGE, solubilized membranes were resolved on 3–12% gradient native PAGE. For 2-D SDS-PAGE, excised lanes from 1-D gels were denatured in 2× SDS sample buffer and resolved on 12% SDS-PAGE containing 8 M urea. Silver staining of 2-D gels was performed as described (42). Representative gel pictures from three independent biological replicates were shown.

High light treatment

Leaf discs excised from the seventh or eighth true leaves of 4-week-old plants were first infiltrated in a solution containing 0.2% (v/v) Tween 20, 1.0 mg ml^{-1} lincomycin, and 0.1 mg ml^{-1} cycloheximide for 15 min, and then transferred to high light conditions (~1000 μmol m^{-2} s^{-1}) for 0, 2, and 4 h. Each sample contains at least five leaf discs, and total proteins were extracted and normalized to tissue fresh weight.

Author contribution—Y. Q., F. Y., and X. L. conceptualization; Y. Q. data curation; Y. Q., F. Y., and X. L. funding acquisition; Y. Q., X. W., P. L., H. L., and L. Y. investigation; Y. Q. and X. W. writing-original draft; Y. Q., F. Y., and X. L. writing-review and editing; X. W. formal analysis; X. W. and P. L. validation; X. W. visualization; J. Z. and X. L. resources; J. M., J. S., and L. A. methodology; X. L. supervision; X. L. project administration.

Acknowledgment—We thank Dr. Aigen Fu of Northwest University in China for kindly providing Cytf and PsaF antibodies.

References

1. Zimorski, V., Ku, C., Martin, W. F., and Gould, S. B. (2014) Endosymbiotic theory for organelle origins. *Curr. Opin. Microbiol.* **22,** 38–48 CrossRef Medline
2. Sato, S., Nakamura, Y., Kaneko, T., Asamizu, E., and Tabata, S. (1999) Complete structure of the chloroplast genome of *Arabidopsis thaliana*. *DNA Res.* **6,** 283–290 CrossRef Medline
3. Leister, D. (2003) Chloroplast research in the genomic age. *Trends Genet.* **19,** 47–56 CrossRef Medline
4. Jarvis, P., and López-Juez, E. (2013) Biogenesis and homeostasis of chloroplasts and other plastids. *Nat. Rev. Mol. Cell Biol.* **14,** 787–802 CrossRef Medline
5. Kleine, T., and Leister, D. (2016) Retrograde signaling: Organelles go networking. *Biochim. Biophys. Acta* **1857,** 1313–1325 CrossRef Medline
6. Taylor, N. L., Tan, Y. F., Jacoby, R. P., and Millar, A. H. (2009) Abiotic environmental stress induced changes in the *Arabidopsis thaliana* chloroplast, mitochondria and peroxisome proteomes. *J. Proteomics* **72,** 367–378 CrossRef Medline
7. Yu, F., Fu, A., Aluru, M., Park, S., Xu, Y., Liu, H., Liu, X., Foudree, A., Nambogga, M., and Rodermel, S. (2007) Variegation mutants and mechanisms of chloroplast biogenesis. *Plant Cell Environ.* **30,** 350–365 CrossRef Medline
8. Nishimura, K., Kato, Y., and Sakamoto, W. (2017) Essentials of proteolytic machineries in chloroplasts. *Mol. Plant* **10,** 4–19 CrossRef Medline
9. Nishimura, K., Kato, Y., and Sakamoto, W. (2016) Chloroplast proteases: Updates on proteolysis within and across suborganellar compartments. *Plant Physiol.* **171,** 2280–2293 CrossRef Medline
10. Chen, M., Choi, Y. D., Voytas, D. F., and Rodermel, S. (2000) Mutations in the Arabidopsis VAR2 locus cause leaf variegation due to the loss of a chloroplast FtsH protease. *Plant J.* **22,** 303–313 CrossRef Medline
11. Sakamoto, W., Tamura, T., Hanba-Tomita, Y., Sodmergen, and Murata, M. (2002) The VAR1 locus of Arabidopsis encodes a chloroplastic FtsH and is responsible for leaf variegation in the mutant alleles. *Genes Cells* **7,** 769–780 CrossRef Medline
12. Yu, F., Park, S., and Rodermel, S. R. (2004) The Arabidopsis FtsH metalloprotease gene family: Interchangeability of subunits in chloroplast oligomeric complexes. *Plant J.* **37,** 864–876 CrossRef Medline
13. Zaltsman, A., Ori, N., and Adam, Z. (2005) Two types of FtsH protease subunits are required for chloroplast biogenesis and photosystem II repair in Arabidopsis. *Plant Cell* **17,** 2782–2790 CrossRef Medline
14. Lindahl, M., Spetea, C., Hundal, T., Oppenheim, A. B., Adam, Z., and Andersson, B. (2000) The thylakoid FtsH protease plays a role in the light-induced turnover of the photosystem II D1 protein. *Plant Cell* **12,** 419–431 CrossRef Medline
15. Kato, Y., Miura, E., Ido, K., Ifuku, K., and Sakamoto, W. (2009) The variegated mutants lacking chloroplastic FtsHs are defective in D1 degradation and accumulate reactive oxygen species. *Plant Physiol.* **151,** 1790–1801 CrossRef Medline
16. Bailey, S., Thompson, E., Nixon, P. J., Horton, P., Mullineaux, C. W., Robinson, C., and Mann, N. H. (2002) A critical role for the Var2 FtsH homologue of *Arabidopsis thaliana* in the photosystem II repair cycle *in vivo*. *J. Biol. Chem.* **277,** 2006–2011 CrossRef Medline
17. Malnoë, A., Wang, F., Girard-Bascou, J., Wollman, F. A., and de Vitry, C. (2014) Thylakoid FtsH protease contributes to photosystem II and cytochrome b6f remodeling in Chlamydomonas reinhardtii under stress conditions. *Plant Cell* **26,** 373–390 CrossRef Medline
18. Järvi, S., Suorsa, M., and Aro, E. M. (2015) Photosystem II repair in plant chloroplasts—regulation, assisting proteins and shared components with photosystem II biogenesis. *Biochim. Biophys. Acta* **1847,** 900–909 CrossRef Medline
19. Chi, W., Sun, X., and Zhang, L. (2012) The roles of chloroplast proteases in the biogenesis and maintenance of photosystem II. *Biochim. Biophys. Acta* **1817,** 239–246 CrossRef Medline
20. Sun, X., Fu, T., Chen, N., Guo, J., Ma, J., Zou, M., Lu, C., and Zhang, L. (2010) The stromal chloroplast Deg7 protease participates in the repair of photosystem II after photoinhibition in Arabidopsis. *Plant Physiol.* **152,** 1263–1273 CrossRef Medline
21. Sun, X., Peng, L., Guo, J., Chi, W., Ma, J., Lu, C., and Zhang, L. (2007) Formation of DEG5 and DEG8 complexes and their involvement in the degradation of photodamaged photosystem II reaction center D1 protein in Arabidopsis. *Plant Cell* **19,** 1347–1361 CrossRef Medline
22. Kato, Y., Miura, E., Matsushima, R., and Sakamoto, W. (2007) White leaf sectors in yellow variegated2 are formed by viable cells with undifferentiated plastids. *Plant Physiol.* **144,** 952–960 CrossRef Medline
23. Park, S., and Rodermel, S. R. (2004) Mutations in ClpC2/Hsp100 suppress the requirement for FtsH in thylakoid membrane biogenesis. *Proc. Natl. Acad. Sci. U.S.A.* **101,** 12765–12770 CrossRef Medline
24. Liu, X., Yu, F., and Rodermel, S. (2010) An Arabidopsis pentatricopeptide repeat protein, SUPPRESSOR OF VARIEGATION7, is required for FtsH-mediated chloroplast biogenesis. *Plant Physiol.* **154,** 1588–1601 CrossRef Medline
25. Putarjunan, A., Liu, X., Nolan, T., Yu, F., and Rodermel, S. (2013) Understanding chloroplast biogenesis using second-site suppressors of immutans and var2. *Photosynth. Res.* **116,** 437–453 CrossRef Medline

26. Hu, F., Zhu, Y., Wu, W., Xie, Y., and Huang, J. (2015) Leaf variegation of thylakoid formation1 is suppressed by mutations of specific sigma-factors in Arabidopsis. *Plant Physiol.* **168,** 1066–1075 CrossRef Medline
27. Adam, Z., Frottin, F., Espagne, C., Meinnel, T., and Giglione, C. (2011) Interplay between N-terminal methionine excision and FtsH protease is essential for normal chloroplast development and function in Arabidopsis. *Plant Cell* **23,** 3745–3760 CrossRef Medline
28. Liu, S., Zheng, L., Jia, J., Guo, J., Zheng, M., Zhao, J., Shao, J., Liu, X., An, L., Yu, F., and Qi, Y. (2019) Chloroplast translation elongation factor EF-Tu/SVR11 is involved in var2-mediated leaf variegation and leaf development in Arabidopsis. *Front. Plant Sci.* **10,** 295 CrossRef Medline
29. Liu, X., Rodermel, S. R., and Yu, F. (2010) A var2 leaf variegation suppressor locus, SUPPRESSOR OF VARIEGATION3, encodes a putative chloroplast translation elongation factor that is important for chloroplast development in the cold. *BMC Plant Biol.* **10,** 287 CrossRef Medline
30. Liu, X., Zheng, M., Wang, R., Wang, R., An, L., Rodermel, S. R., and Yu, F. (2013) Genetic interactions reveal that specific defects of chloroplast translation are associated with the suppression of var2-mediated leaf variegation. *J. Integr. Plant Biol.* **55,** 979–993 CrossRef Medline
31. Qi, Y., Zhao, J., An, R., Zhang, J., Liang, S., Shao, J., Liu, X., An, L., and Yu, F. (2016) Mutations in circularly permuted GTPase family genes AtNOA1/RIF1/SVR10 and BPG2 suppress var2-mediated leaf variegation in *Arabidopsis thaliana*. *Photosynth. Res.* **127,** 355–367 CrossRef Medline
32. Yu, F., Liu, X., Alsheikh, M., Park, S., and Rodermel, S. (2008) Mutations in SUPPRESSOR OF VARIEGATION1, a factor required for normal chloroplast translation, suppress var2-mediated leaf variegation in Arabidopsis. *Plant Cell* **20,** 1786–1804 CrossRef Medline
33. Yu, F., Park, S. S., Liu, X., Foudree, A., Fu, A., Powikrowska, M., Khrouchtchova, A., Jensen, P. E., Kriger, J. N., Gray, G. R., and Rodermel, S. R. (2011) SUPPRESSOR OF VARIEGATION4, a new var2 suppressor locus, encodes a pioneer protein that is required for chloroplast biogenesis. *Mol. Plant* **4,** 229–240 CrossRef Medline
34. Zheng, M., Liu, X., Liang, S., Fu, S., Qi, Y., Zhao, J., Shao, J., An, L., and Yu, F. (2016) Chloroplast translation initiation factors regulate leaf variegation and development. *Plant Physiol.* **172,** 1117–1130 Medline
35. Costanzo, M., VanderSluis, B., Koch, E. N., Baryshnikova, A., Pons, C., Tan, G., Wang, W., Usaj, M., Hanchard, J., Lee, S. D., Pelechano, V., Styles, E. B., Billmann, M., van Leeuwen, J., van Dyk, N., *et al.* (2016) A global genetic interaction network maps a wiring diagram of cellular function. *Science* **353,** aaf1420 CrossRef Medline
36. Wang, R., Zhao, J., Jia, M., Xu, N., Liang, S., Shao, J., Qi, Y., Liu, X., An, L., and Yu, F. (2018) Balance between cytosolic and chloroplast translation affects leaf variegation. *Plant Physiol.* **176,** 804–818 CrossRef Medline
37. Chen, G., Bi, Y. R., and Li, N. (2005) EGY1 encodes a membrane-associated and ATP-independent metalloprotease that is required for chloroplast development. *Plant J.* **41,** 364–375 CrossRef Medline
38. Li, B., Li, Q., Xiong, L., Kronzucker, H. J., Krämer, U., and Shi, W. (2012) Arabidopsis plastid AMOS1/EGY1 integrates abscisic acid signaling to regulate global gene expression response to ammonium stress. *Plant Physiol.* **160,** 2040–2051 CrossRef Medline
39. Rudner, D. Z., Fawcett, P., and Losick, R. (1999) A family of membrane-embedded metalloproteases involved in regulated proteolysis of membrane-associated transcription factors. *Proc. Natl. Acad. Sci. U.S.A.* **96,** 14765–14770 CrossRef Medline
40. Weihofen, A., and Martoglio, B. (2003) Intramembrane-cleaving proteases: Controlled liberation of proteins and bioactive peptides. *Trends Cell Biol.* **13,** 71–78 CrossRef Medline
41. Guo, D., Gao, X., Li, H., Zhang, T., Chen, G., Huang, P., An, L., and Li, N. (2008) EGY1 plays a role in regulation of endodermal plastid size and number that are involved in ethylene-dependent gravitropism of light-grown Arabidopsis hypocotyls. *Plant Mol. Biol.* **66,** 345–360 CrossRef Medline
42. Järvi, S., Suorsa, M., Paakkarinen, V., and Aro, E. M. (2011) Optimized native gel systems for separation of thylakoid protein complexes: Novel super- and mega-complexes. *Biochem. J.* **439,** 207–214 CrossRef Medline
43. Wang, F., Qi, Y., Malnoë, A., Choquet, Y., Wollman, F. A., and de Vitry, C. (2017) The high light response and redox control of thylakoid FtsH protease in *Chlamydomonas reinhardtii*. *Mol. Plant* **10,** 99–114 CrossRef Medline
44. Costanzo, M., Kuzmin, E., van Leeuwen, J., Mair, B., Moffat, J., Boone, C., and Andrews, B. (2019) Global genetic networks and the genotype-to-phenotype relationship. *Cell* **177,** 85–100 CrossRef Medline
45. Barry, C. S., Aldridge, G. M., Herzog, G., Ma, Q., McQuinn, R. P., Hirschberg, J., and Giovannoni, J. J. (2012) Altered chloroplast development and delayed fruit ripening caused by mutations in a zinc metalloprotease at the lutescent2 locus of tomato. *Plant Physiol.* **159,** 1086–1098 CrossRef Medline
46. Zhang, S., Zhi, H., Li, W., Shan, J. G., Tang, C. J., Jia, G. Q., Tang, S., and Diao, X. M. (2018) SiYGL2 is involved in the regulation of leaf senescence and photosystem II efficiency in *Setaria italica* (L.) P. Beauv. *Front. Plant Sci.* **9,** 1308 CrossRef Medline
47. Yu, F. W., Zhu, X. F., Li, G. J., Kronzucker, H. J., and Shi, W. M. (2016) The chloroplast protease AMOS1/EGY1 affects phosphate homeostasis under phosphate stress. *Plant Physiol.* **172,** 1200–1208 CrossRef Medline
48. Eberhard, S., Finazzi, G., and Wollman, F. A. (2008) The dynamics of photosynthesis. *Annu. Rev. Genet.* **42,** 463–515 CrossRef Medline
49. Murata, N. (2009) The discovery of state transitions in photosynthesis 40 years ago. *Photosynth. Res.* **99,** 155–160 CrossRef Medline
50. Aro, E. M., Virgin, I., and Andersson, B. (1993) Photoinhibition of photosystem II. Inactivation, protein damage and turnover. *Biochim. Biophys. Acta* **1143,** 113–134 CrossRef Medline
51. Neff, M. M., Neff, J. D., Chory, J., and Pepper, A. E. (1998) dCAPS, a simple technique for the genetic analysis of single nucleotide polymorphisms: experimental applications in *Arabidopsis thaliana* genetics. *Plant J.* **14,** 387–392 CrossRef Medline
52. Clough, S. J., and Bent, A. F. (1998) Floral dip: A simplified method for Agrobacterium-mediated transformation of *Arabidopsis thaliana*. *Plant J.* **16,** 735–743 CrossRef Medline